Check for updates

Journal of Extracellular Biology

TECHNICAL REPORT OPEN ACCESS

Workflow for the Isolation and Characterisation of Human Milk Extracellular Vesicles (HMEVs) and Their Inflammatory Biomarker Profile

Jose Luis Moreno-Casillas[1,2] | Laura Ripoll-Seguer[1,2] | Isabel Ten-Doménech[3,4] | Marta Gómez-Ferrer[5] | Pilar Sepúlveda[5,6,7,8] | Abel Albiach-Delgado[2,3] | Juan Daniel Sanjuan-Herráez[9] | María Gormaz[3,10] | David Pérez-Guaita[4] | Bernhard Lendl[11] | María Cernada[3,10] | Guillermo Quintás[9] | Julia Kuligowski[2,3]

[1]Neonatal Research Group, Health Research Institute La Fe (IIS La Fe), Valencia, Spain | [2]Servicio de Análisis de Vesículas Extracelulares (SAVE), Health Research Institute La Fe (IIS La Fe), Valencia, Spain | [3]Spanish Network in Maternal, Neonatal, Child and Developmental Health Research (RICORS- SAMID) (RD24/0013/0014), Neonatal Research Group, Health Research Institute La Fe, Valencia, Spain | [4]Department of Analytical Chemistry, University of Valencia, Burjassot, Spain | [5]Regenerative Medicine and Heart Transplantation Unit, Health Research Institute La Fe (IIS La Fe), Valencia, Spain | [6]Centro de Investigación Biomédica en Red Enfermedades Cardiovasculares (CIBERCV), Carlos III Institute of Health, Madrid, Spain | [7]Cardiology Service, University & Polytechnic Hospital La Fe, Valencia, Spain | [8]Department of Pathology, University of Valencia, Valencia, Spain | [9]Health and Biomedicine, Leitat Technological Center, Terrassa, Spain | [10]Division of Neonatology, University & Polytechnic Hospital La Fe, Valencia, Spain | [11]Institute of Chemical Technologies and Analytics, Technische Universität Wien, Vienna, Austria

Correspondence: Julia Kuligowski (julia.kuligowski@uv.es; julia_kuligowski@iislafe.es)

Received: 1 August 2025 | **Revised:** 26 December 2025 | **Accepted:** 29 December 2025

Keywords: inflammatory biomarker | newborn | nutrition | oxidised lipids | oxylipins | preterm infant | ultra-performance liquid chromatography–tandem mass spectrometry (UPLC-MS/MS)

ABSTRACT

Human milk extracellular vesicles (HMEVs), secreted by mammary epithelial cells, are enriched in bioactive molecules that support intestinal epithelial integrity. Among these, oxylipins, that is, lipid mediators derived from polyunsaturated fatty acids, are gaining interest for their immunomodulatory and neuroprotective functions in breastfed infants. However, current workflows for oxylipin profiling in HMEVs often lack sensitivity or breadth, limiting mechanistic insights. This study presents an optimised workflow for comprehensive oxylipin profiling in HMEVs. HMEVs were isolated via size-exclusion chromatography and ultracentrifugation, followed by characterisation using attenuated total reflectance–Fourier transform infrared spectroscopy, Western blotting, Exoview immunocapture, tunable resistive pulse sensing and transmission electron microscopy. The influence of different pre-analytical protocols on HMEV recovery was assessed. Cryolysis with liquid nitrogen was employed for vesicle lysis before targeted oxylipin quantification using ultra-performance liquid chromatography–tandem mass spectrometry. The analysis of 10 human milk samples revealed 9,10-DiHOME, 12,13-DiHOME and 11,12-EET as the most abundant oxylipins, with concentrations ranging from 0.5 to 3.7, 0.8 to 4.5 and 0.1 to 0.3 nM, respectively. This refined pipeline enables in-depth oxylipin profiling in HMEVs and serves as a robust platform for future in vitro and in vivo investigations into EV-mediated lipid signalling.

1 | Introduction

Necrotising enterocolitis (NEC) is a severe gastrointestinal disorder that primarily affects premature neonates, resulting in inflammation and necrosis of intestinal tissue through mechanisms that remain poorly understood (Niño et al. 2016). Human milk (HM) proactive components, including extracellular vesicles (EVs), are believed to play a critical role in mitigating the risk

This is an open access article under the terms of the Creative Commons Attribution-NonCommercial-NoDerivs License, which permits use and distribution in any medium, provided the original work is properly cited, the use is non-commercial and no modifications or adaptations are made.
© 2026 The Author(s). *Journal of Extracellular Biology* published by Wiley Periodicals, LLC on behalf of the International Society for Extracellular Vesicles.

of NEC, though their exact mechanisms remain to be fully elucidated (Pisano et al. 2020; Chen et al. 2021; Yan et al. 2022; Wang et al. 2019). Human milk extracellular vesicles (HMEVs) carry bioactive molecules, including lipids, proteins and RNA, that are essential for immune modulation, coagulation support and the enhancement of intestinal barrier function (Vahkal et al. 2024; Chutipongtanate et al. 2022). Notably, HMEVs show resistance to digestion, allowing their bioactive contents to reach the infant's intestinal tract intact, thereby underscoring their potential to reduce NEC (Zhou et al. 2012; Herwijnen et al. 2018; Kahn et al. 2018; Yung et al. 2024; Liao et al. 2017; Tong et al. 2023).

Oxylipins such as linoleic acid-derived 9,10-DiHOME and 12,13-DiHOME and oxidised omega-3 metabolites are present in HMEVs. They are known for their antiinflammatory and proresolutive effects, supporting inflammation resolution and enhancing intestinal integrity, both critical for neonatal health (Gómez-Ferrer et al. 2023; Spector and Norris 2007; Wang et al. 2018). Recent research on the oxylipin profile of HMEVs highlights their role in regulating gut inflammation (Gómez-Ferrer et al. 2023). As potent modulators of inflammation, oxidised lipids hold promise for preventing neonatal intestinal disorders, including NEC (Burge et al. 2021).

Although some methods allow direct analysis of HMEVs in liquid samples, isolation is often necessary for detailed characterisation and clinical research. However, EVs' isolation remains challenging due to the complexity of the HM matrix (Hu et al. 2021). Differential ultracentrifugation (dUC), including variant density gradient ultracentrifugation (DGUC), is recognised as the gold-standard EV isolation technique. This is due to its ability to achieve high-purity isolates by sequentially removing cells, debris and apoptotic bodies (Robinson et al. 2023; Welsh et al. 2024), and separating vesicles based on size, density and mass (Li et al. 2022; Ter-Ovanesyan et al. 2021). DGUC enhances purity by using sucrose or iodixanol gradients to separate EVs based on density; however, contamination from lipoproteins and other similarly dense molecules may still be a challenge (Yuana et al. 2014). Despite their widespread use, both dUC and DGUC are labour-intensive, require large sample volumes and face challenges with respect to lipoprotein coisolation (Nordin et al. 2015; Grätz et al. 2024). Alternative isolation techniques such as size-exclusion chromatography (SEC), ultrafiltration and flow field-flow fractionation have been proposed to overcome these limitations, along with other methods like ion-exchange chromatography, electrophoresis and immunoaffinity capture (Liangsupree et al. 2021). Among these techniques, SEC stands out for its simplicity, scalability and its ability to preserve vesicle integrity while efficiently separating EVs from soluble proteins and minimising lipoprotein contamination (Sidhom et al. 2020). In practical terms, SEC scalability refers to its adaptability to different column formats and processing volumes, allowing the handling of samples spanning from a few to up to 100 mL of loading volume. This flexibility allows SEC-based protocols to be applied both to small research samples and to larger clinical or biobank-scale studies, overcoming one of the main limitations of ultracentrifugation-based methods. Moreover, SEC-based EV isolation relies on a hydrodynamic size-based separation, making it particularly effective for processing lipid-rich and complex biological matrices such as milk (Benedikter et al. 2017; Oeyen et al. 2018). Recent studies indicate that combining SEC with UC further enhances EV yield and purity by removing larger contaminants, such as caseins and remaining lipoproteins, while concentrating EVs (Simon et al. 2020; Takov et al. 2019; Guerreiro et al. 2018).

In addition, special care should also be given to sample handling. According to the MISEV 2023 guidelines, HM should undergo prestorage processing, including the removal of cellular debris, to minimise contaminants and prevent sample degradation (Welsh et al. 2024). Then, isolated EVs should be stored at −80°C to preserve their structural integrity and cargo. The addition of butylated hydroxytoluene (BHT) during HM processing can help to prevent lipid oxidation, ensuring a more accurate representation of the lipidomic profile in subsequent analysis (Sokolova et al. 2011). Although the importance of freezing conditions is well-documented, the impact of BHT in maintaining oxylipin stability in HMEVs has not been studied so far. Given that HMEVs represent a relatively recent area of research and considering the complexity and variability of current sample handling methods, the number of integrated protocols or methods for the isolation and analysis of HMEVs is scarce, particularly for downstream metabolomic or lipidomic profiling requiring prior vesicle lysis.

This study presents a combined SEC-dUC workflow for obtaining highly purified HMEV extracts, optimised for clinical studies. The workflow includes the characterisation of isolated HMEVs with different techniques, including ultra-performance liquid chromatography–tandem mass spectrometry (UPLC-MS/MS) for oxylipin screening after HMEV lysis. This protocol enables, for the first time, the detection of potent antiinflammatory and neuroprotective oxylipins, including arachidonic acid-derived epoxyeicosatrienoic acids (EETs) (Gómez-Ferrer et al. 2023; Spector and Norris 2007; Wang et al. 2018) in HMEVs.

2 | Material and Methods

2.1 | Standards and Reagents

Methanol (MeOH), acetonitrile (ACN), ethanol (EtOH) and ethyl acetate (EtOAc) of LC-MS grade were acquired from Scharlau (Spain). Glycerol, isopropanol (IPA), BHT, formic acid, acetic acid (HAc), sodium acetate (NaAc), calcium chloride ($CaCl_2$), potassium dihydrogen phosphate (KH_2PO_4) and hydrochloric acid (HCl) were obtained from Sigma–Aldrich Química SL (Spain) with purities of analytical grade or higher. RIPA buffer and protease inhibitor (Complete Mini and PhosSTOP) were purchased from Sigma–Aldrich (Germany). Laemmli sample buffer 4×, 2-mercaptoethanol, 4%–20% Mini-Protean TGX Gel, Tris/Glycine/SDS buffer, PVDF membrane and TBS with 0.1% Tween-20 were purchased from BioRad (France). Albumin standard was obtained from Sigma–Aldrich (Barcelona, Spain). Primary antibodies against CD81, Alix, β-casein and secondary antibody against IgG were purchased from Santa Cruz Biotech (USA). Supersignal West Femto was purchased from Thermo Fisher Scientific (Spain). Oxylipins standards (i.e., 12,13-DiHOME, 9,10-DiHOME, 18-HEPE, 17,18-DiHETE, 8(S),15(S)-DiHETE, 14,15-DiHETE, 14-HDHA/14-HDoHE, 17-HDHA/17-HDoHE, 19,20-DiHDPA, PGE_2, Maresin-2, PDX, TXB_2, LTB_4, $PGF_{2\alpha}$, 5,6-EET, 14,15-EET, 11,12-EET, 8,9-EET, 8,9-DiHET, 14,15-DiHET, 5,6-DiHET and 11,12-DiHET) and deuterated internal

27682811, 2026, 1, Downloaded from https://isevjournals.onlinelibrary.wiley.com/doi/10.1002/jex2.70110 by Spanish Cochrane National Provision (Ministerio de Sanidad), Wiley Online Library on [11/03/2026]. See the Terms and Conditions (https://onlinelibrary.wiley.com/terms-and-conditions) on Wiley Online Library for rules of use; OA articles are governed by the applicable Creative Commons License

standards (IS) (i.e., $PGF_{2\alpha}$-D_4, 12,13-DiHOME-D_4, Maresin 2-D_5, 9,10-DiHOME-D_{11} and 14,15-DiHET-D_{11}) were acquired from Cayman Chemicals (Ann Arbour, MI, USA) (full names for abbreviations are shown in Table S1). Ultrapure water was generated with a Milli-Q Integral Water Purification System (Merck Millipore, Darmstadt, Germany). Leprechaun Exosome Human Tetraspanin kits with CD63, CD81 and CD9 immobilised antibodies were supplied by Izasa Scientific (Barcelona, Spain). For SEC isolation, qEVoriginal 35 nm (qEV10) columns (Izon Science, Christchurch, New Zealand; 10 mL bed volume) were used. NP150 nanopores and carboxylate polystyrene calibration particles (CPC200, Izon Science Europe Ltd, Lyon, France) were employed for tunable resistive pulse sensing (TRPS) measurements.

2.2 | HM Clean-Up and Sample Collection

The study protocol was approved by the Ethics Committee for Biomedical Research of the Health Research Institute La Fe (Valencia, Spain) with approval number #2022-922-1. All procedures were carried out in compliance with the Declaration of Helsinki. The volunteers were enrolled at the Human Milk Bank of the University & Polytechnic Hospital La Fe (Valencia, Spain). Volunteers gave their informed consent for inclusion before being enrolled in the study. Demographic (maternal age, infant's sex, gestational age and postnatal age) and anthropometric (birth weight, length and head circumference) data from mothers and their infants are summarised in Table S2. HM was collected following the guidelines provided by hospital personnel, which involved several steps: (i) Thorough hand washing with water and soap for at least 15 s, followed by drying with a clean towel and sanitisation using hand sanitiser. (ii) Cleansing of the skin area in contact with the milk pump with water and drying using sterile gauzes. No creams or ointments were to be applied to the skin before HM extraction; if any had been used, the skin was to be carefully cleaned with water and soap. (iii) Extraction of HM using a clean and sterilised HM pump into sterile bottles. Milk was collected from donors into sterile containers during a single day (8 a.m.–3 p.m.). Each donor provided milk from a single full expression, and samples were kept on ice immediately after collection. For the pooled workflow optimisation experiment, all fresh samples collected within this time window were processed directly upon arrival in the laboratory and combined into one 180 mL pooled sample. After pooling, each milk fraction was processed as detailed in Figure 1. For donor-specific oxylipin analyses, 7 mL HM aliquots of 10 individual donors were skimmed by centrifugation and stored at −80°C until analysis. All donors provided mature HM, including 8 term and 2 preterm deliveries.

2.3 | HM Clean-Up, Storage and EV Isolation

For fresh, skimmed HM clean-up, four casein removal protocols (CRPs) were tested (Kunz and Lönnerdal 1989; Ten-Doménech et al. 2018): In CRP1, 1.5 mL was treated with 180 µL of a 10% (v/v) HAc/NaAc solution (pH 4.6), shook for 10 min and incubated in a Thermo Shaker Biosan TS-100C for 20 min at 4°C. Then, 38 µL of 2 M $CaCl_2$ was added, and the mixture was shaken for 30 min at 500 rpm at 4°C, followed by centrifugation at 12,300 × *g* for 10 min at 4°C. In CRP2, 1.5 mL was mixed with 45 µL of 2 M $CaCl_2$ and 45 µL of 0.5 M KH_2PO_4 (pH 6.0), shook and centrifuged at 12,300 × *g* for 10 min at 4°C. In CRP3, 5 mL was diluted 1:1 with ultrapure water, the pH adjusted to 4.3 with 1 M HCl, shook for 5 min and centrifuged at 5100 × *g* for 20 min at 4°C. Finally, in CRP4, 1.5 mL was treated with 180 µL of 10% (v/v) HAc, shook for 10 min, incubated for 20 min at 4°C and centrifuged at 12,300 × *g* for 10 min at 4°C.

To assess the impact of HM storage (HMS) on HMEVs, direct processing (HM-DP) and two storage methods (HMS1 and HMS2) were compared using an SEC-dUC EVs isolation method. Figure 1 gives an overview of the tested HMEV isolation approaches. Additionally, results using HMS2 combined with dUC (HMS2-dUC) for EV-isolation were included as reference to facilitate the analysis of the impact of the isolation method on the retrieved HMEV data. For HM-DP, fresh HM was processed without freezing and centrifuged twice at 3000 × *g* for 10 min at room temperature (RT) to remove fat and cells. In HMS1 approach, HM was stored at −80°C and skimmed after defrosting prior to EV isolation. HMS2 involved skimming of HM (3000 × g, 10 min, RT) and then storage at −80°C until further processing. These approaches assessed whether the timing of freezing before or after skimming influenced sample quality, with HM-DP serving as control.

Two HMEVs isolation methods based on dUC and SEC-dUC were assessed. A detailed description of the dUC method can be found elsewhere (Ramos-Garcia et al. 2021). The SEC-dUC method included additional centrifugation steps at 5000 × *g* for 30 min at 4°C and 10,000 × *g* for 30 min at 4°C, protein precipitation by1:1 dilution with Milli-Q water, pH adjustment to 4.3 with 1 M HCl and centrifugation at 5100 × *g* for 20 min at 4°C. Then, the supernatant was filtered (0.45 µm syringe filter). HMEVs were isolated using SEC and an automatic fraction collector (AFCV1, IZON Europe Ltd). The first four HMEV-enriched collected fractions were pooled, ultracentrifuged at 175,000 × *g* for 2 h at 4°C, resuspended in 200 µL of PBS and stored at −80°C until analysis.

For the evaluation of the different sample storage, clean up and EV isolation methods, a pool of donor HM from different mothers was employed. Analyses were performed in triplicate with initial sample volumes of 7 mL for methods employing HM-DP, HMS1 and HMS2, combined with SEC-dUC and 25 mL for the HMS2-dUC approach.

2.4 | Quality Control of Isolated HMEVs

2.4.1 | Attenuated Total Reflectance–Fourier Transform Infrared (ATR-FTIR) Spectroscopy

As described previously (Ramos-Garcia et al. 2021), ATR-FTIR spectra were obtained in the 4000–400 cm^{-1} range with a resolution of 4 cm^{-1} for the acquisition of HMEVs fingerprints. An Alpha II spectrometer (Bruker Optics GmbH, Ettlingen, Germany) equipped with a temperature-stabilised deuterated triglycine sulphate detector, a CenterGlow IR source and a platinum ATR with a monolithic single reflection diamond was used for the measurements. OPUS software (Bruker Optics GmbH, Ettlingen, Germany) was used to control the spectrophotometer.

27682811, 2026, 1, Downloaded from https://isevjournals.onlinelibrary.wiley.com/doi/10.1002/jex2.70110 by Spanish Cochrane National Provision (Ministerio de Sanidad), Wiley Online Library on [11/03/2026]. See the Terms and Conditions (https://onlinelibrary.wiley.com/terms-and-conditions) on Wiley Online Library for rules of use; OA articles are governed by the applicable Creative Commons License

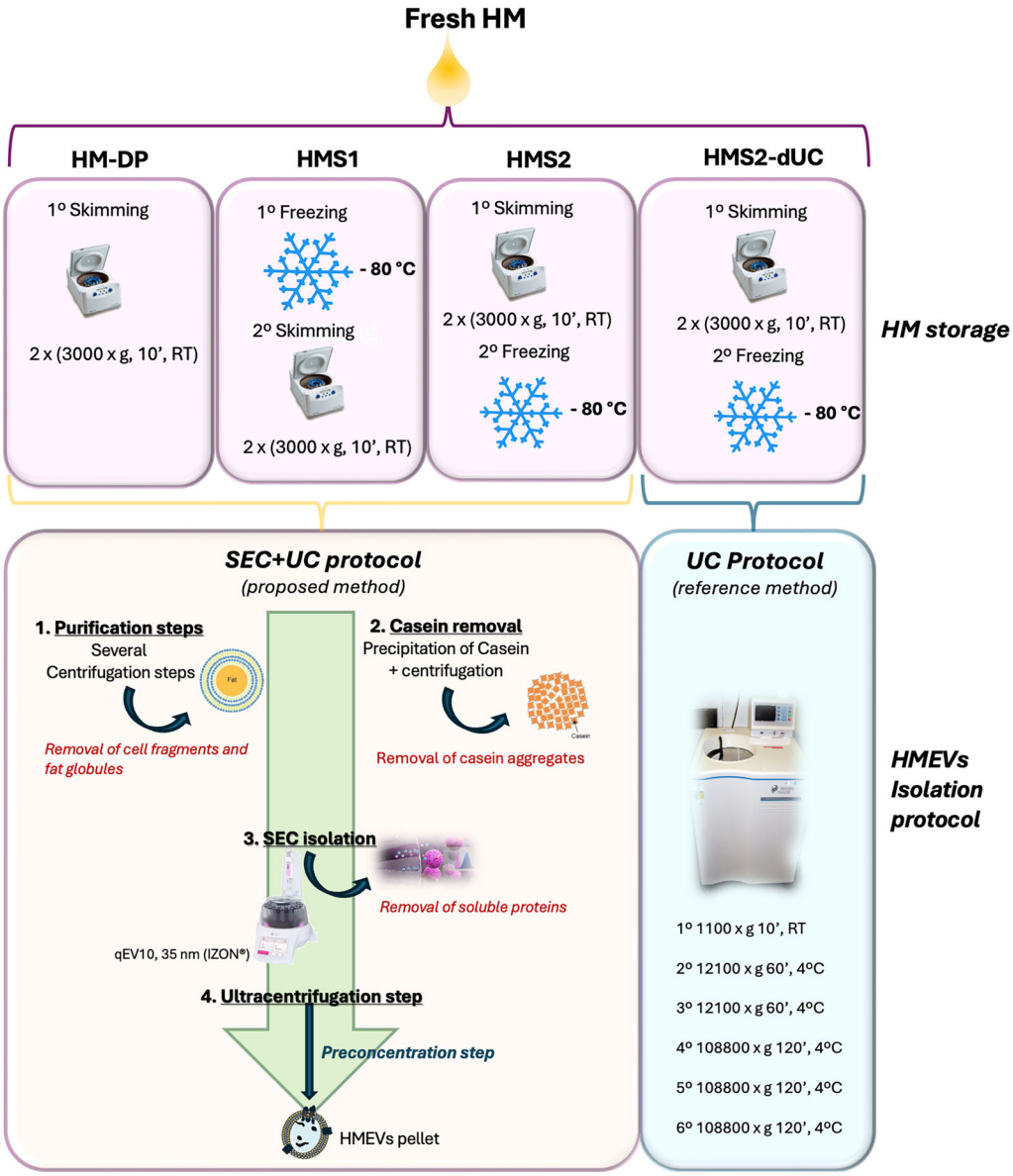


FIGURE 1 | Overview of the tested workflows combining different types of HM storage, clean-up and HMEVs isolation approaches. HM, human milk; HMEVs, human milk extracellular vesicles.

A 2 µL aliquot of the EV suspension was placed on the ATR crystal using a micropipette and left to dry for 5 min at RT. The spectra were collected by averaging 32 scans, using a previously recorded air spectrum under identical conditions as a background. The ATR crystal was thoroughly cleaned after each sample using Milli-Q water to fully restore the baseline signal. The protein content was quantified by integrating the area of the Amide I band in the 1724–1591 cm^{-1} region, using an external calibration curve and serial dilutions of albumin standards ranging from 0 to 6 g/L. Additionally, purity was estimated as particle-to-protein ratio (particle/protein).

2.4.2 | Western Blot Analysis

HMEV suspension containing 30 µg of total protein was lysed in RIPA buffer with protease inhibitors, followed by the addition of Laemmli sample buffer containing 2-mercaptoethanol. Samples were denatured at 90°C during 5 min. Proteins were separated on a 4%–20% Mini-Protean TGX Gel and run at 150 V in Tris/Glycine/SDS buffer for 1 h. Proteins were transferred to a PVDF membrane during 3 h. The membrane was blocked in TBS with 0.1% Tween-20 for 90 min at RT. The membrane was incubated overnight at 4°C with human primary antibodies: anti-CD81 (dilution 1/500; Santa Cruz Biotech, B-11), anti-Alix (dilution 1/500; Santa Cruz Biotech, 3A9) and anti-β casein (dilution 1/500; Santa Cruz Biotech, F20.14). Then, membranes were incubated for 60 min with secondary antibody mouse anti-mIgG (dilution 1/10,000, Santa Cruz Biotech, FC BP-HRP). Detection was carried out using SuperSignal West Femto and Amersham Imager 600 (GE Healthcare, Chicago, IL, USA) and quantified with ImageJ software (NIH, Bethesda, MD, USA).

27682811, 2026, 1, Downloaded from https://isevjournals.onlinelibrary.wiley.com/doi/10.1002/jex2.70110 by Spanish Cochrane National Provision (Ministerio de Sanidad), Wiley Online Library on [11/03/2026]. See the Terms and Conditions (https://onlinelibrary.wiley.com/terms-and-conditions) on Wiley Online Library for rules of use; OA articles are governed by the applicable Creative Commons License

2.4.3 | Membrane Protein Colocalisation Analysis

For HMEV tetraspanin colocalisation analysis, the ExoView R200+ platform (NanoView Biosciences, Brighton, USA) was employed, using 'Leprechaun Exosome Human Tetraspanin' kits with immobilised CD63, CD81 and CD9 antibodies. The chips were prepared following the manufacturer's instructions using the buffers provided with the kit. Isolated HMEVs were incubated overnight at RT, with 50 μL of samples diluted 1:100 or 1:1000 added to each chip, in accordance with the manufacturer's instructions. Fluorescent antibodies against CD9, CD63 and CD81 were applied to detect captured HMEVs and study tetraspanin colocalisation profiles.

2.4.4 | TRPS

The Exoid system (IZON Europe Ltd) was employed for particle count and size distribution analysis of HMEVs. Two different nanopores (NP150 and NP250, IZON Europe Ltd) were used, being able to study a size range from 80 to 500 nm. General pressure of 1000 Pa was applied, and a nanopore stretch from 46 to 48 mm was required depending on the size range. Size and particle concentration were determined by comparing the resistive pulses (i.e., blockade rate) between isolated HMEVs and carboxylated polystyrene calibration particles (CPC200, $8.2{\cdot}10^{11}$ particles/mL, 200 nm). Calibration standard particles and samples were diluted 1:1000 and 1:800 in fresh, filtered PBS (1×), respectively. Calibration and sample measurements were performed employing the same pressure, voltage and nanopore stretch, measuring at least 500 particles. with two different pressures. Data analysis was carried out with Izon Control Suite software (version 1.0.2.32, Izon Europe Ltd).

2.4.5 | Transmission Electron Microscopy (TEM)

The Glow Discharge process was carried out on the grids, and 5 μL of isolated HMEVs were deposited and contrasted with uranyl acetate. They were observed on the Hitachi HT-7800 where the images were acquired with the 20 Mpx Xarosa camera.

2.5 | Oxylipin Analysis

Four HMEVs lysis strategies (EVLSs) (Melero-Fernandez de Mera et al. 2022; Anaya et al. 2019) were tested: In EVLS1, 200 μL of HMEV extract was mixed with 200 μL of cold MeOH (−20°C), vortexed for 30 s, sonicated in an ice/water bath for 17 min and centrifuged at 160,000 × *g* for 20 min at 4°C; the supernatant was collected, and the pellet resuspended in 100 μL of cold MeOH and combined with the supernatant. The second lysis strategy (EVLS2) differed from EVLS1 by the use of cold ACN (−20°C) instead of MeOH. EVLS3 differed from ELS1 by the inclusion of three freeze/thaw cycles in liquid nitrogen after sonication. Finally, EVLS4 differed from EVLS2 by the use of three additional freeze/thaw cycles in liquid nitrogen after sonication. To evaluate lysis efficiency, lysed extracts were diluted with 1X PBS to 25 mLand ultracentrifuged at 175,000 × *g* for 2 h at 4°C, resuspending the resulting pellets in 200 μL of 1X PBS. Extracts and a PBS blank (i.e., control) were stained with 5 μM carboxyfluorescein diacetate succinimidyl diester (CFSE) for 15 min at 37°C, followed by UC to remove excess CFSE. Fluorescence was measured using a Synergy H1 plate reader (BioTek) at excitation/emission wavelengths of 495/515 nm.

For the optimisation of the SPE-UPLC-MSMS method for oxylipins analysis, 1200 μL of a pooled HMEV lysed extract was thawed on ice, homogenised and mixed with 30 μL of a 500 nM oxylipins standard solution and 30 μL of a solution containing 1.25 μM of IS (a full list of included oxylipins and ISs can be found in Section 2.1), along with 30 μL of BHT (10 mg/mL in EtOH). Two SPE procedures were evaluated using 200 μL aliquots of the extract in triplicate to evaluate extraction efficiency. The first SPE method used Oasis MAX columns as reported elsewhere (Albiach-Delgado et al. 2024). The second SPE method used Oasis HLB columns, where 200 μL aliquots were mixed with 200 μL MeOH (0.1% v/v formic acid), incubated at 4°C for 10 min and centrifuged at 3500 × *g* for 10 min. The supernatant was diluted to 1.4 mL with water and loaded onto preconditioned columns (1 mL EtOAc, 1 mL MeOH, 1 mL water with 0.1% formic acid and 5% MeOH). After loading the sample, columns were washed with 1 mL of the same water solution and eluted with 250 μL MeOH followed by three 250 μL aliquots of EtOAc. Extracts were evaporated using a miVac centrifugal vacuum concentrator (Genevac LTD, Ipswich, UK) and reconstituted in 50 μL MeOH/water (50:50).

For oxylipin analysis of study samples, 175 μL of BHT (10 mg/mL in EtOH) was added to 7 mL of skimmed HM samples before storage. After isolation and lysis, 200 μL of HMEVs extract was thawed, homogenised and mixed with 5 μL of the IS solution and 5 μL of BHT (10 mg/mL in EtOH). Samples were processed using the optimised Oasis HLB method, evaporated and reconstituted in 50 μL MeOH/water (50:50).

Extracts were analysed using an Acquity-Xevo TQ-XS UPLC-MS/MS system (Waters, Milford, MA, USA), as described elsewhere (Albiach-Delgado et al. 2024). Separations were achieved on a Waters Acquity UPLC BEH C18 column (2.1 × 100 mm, 1.7 μm) employing a binary gradient of 0.1% v/v HAc (mobile Phase A) and ACN:IPA (90:10, v/v) (mobile Phase B). Column temperature, flow rate and injection volume were set to 40°C, 0.6 mL/min and 5 μL, respectively. The gradient program spanned 10.0 min: from 0.0 to 1.0 min, 75% B; from 1.0 to 8.0 min, B increased up to 95%; from 8.0 to 8.5 min, 95% B; and from 8.51 to 10.0 min, B decreased to 75%, followed by a 1.5-min reequilibration at 75% B. MS detection operated in negative electrospray ionisation mode with source and desolvation temperatures of 150 and 600°C, and nitrogen cone and desolvation gas flows of 150 and 1000 L/h. Dwell time was set to obtain at least 10 data points per peak. Sample extracts were injected twice for oxylipin quantitation and semiquantification of additional compounds. Quantification involved linear regression curves with $1/x$ weighting and IS signal normalisation, while semiquantification was based on peak area comparison.

2.6 | Data Acquisition and Analysis

For ATR-FTIR spectra acquisition, the OPUS 8.5 software (Bruker Optics GmbH) was used. Tetraspanin colocalisation data acquisi-

27682811, 2026, 1, Downloaded from https://isevjournals.onlinelibrary.wiley.com/doi/10.1002/jex2.70110 by Spanish Cochrane National Provision (Ministerio de Sanidad), Wiley Online Library on [11/03/2026]. See the Terms and Conditions (https://onlinelibrary.wiley.com/terms-and-conditions) on Wiley Online Library for rules of use; OA articles are governed by the applicable Creative Commons License

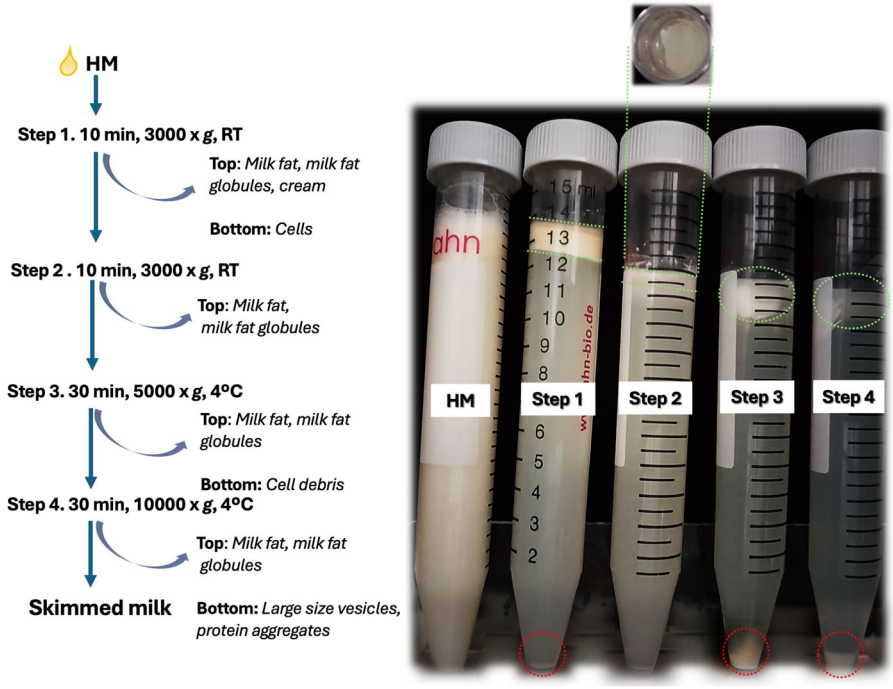


FIGURE 2 | Preprocessing steps applied before the isolation of human milk extracellular vesicles (HMEVs). The green and red dashed circles highlight the upper fat layer and the bottom pellet, respectively.

tion and analysis were carried out using the ExoView analyser software (version 3.1.4) from NanoView. UPLC-MS/MS data acquisition and oxylipin profiling were conducted with MassLynx software (version 4.2) by Waters. Statistical analysis was performed utilising the PLS Toolbox (version 8.7.1) from Eigenvector Research Inc. (Wenatchee, USA), operating in MATLAB 2021b (Mathworks Inc., Natick, MA, USA), along with MATLAB's integrated functions and locally developed scripts. All relevant information on the performed experiments has been submitted to the EV-TRACK knowledgebase (EV-TRACK Consortium et al. 2017) (EV-TRACK ID: EV250084).

3 | Results and Discussion

3.1 | HMEV Isolation

Raw milk contains a diverse mixture of particles, including EVs, casein micelles, milk fat globules and cells. Due to the complexity of the HM matrix, before isolating EVs from milk, several preprocessing steps are required, as shown in Figure 2. Initially, centrifugation is used to remove fat, milk fat globules, cells and cell debris. Due to their low density, fat and milk fat globules rise to the top, forming a distinct layer, while cells and cell debris settle at the bottom as a pellet. EVs and casein micelles remain in the intermediate layer between the fat layer and the pellet (Hu et al. 2021; Anaya et al. 2019; Yamauchi et al. 2019).

In Step 1, centrifugation at 3000 × *g* for 10 min at RT results in the formation of a thick layer of fat on the tube's surface, while cells settle at the bottom. The intermediate layer is then subjected to Step 2, performed under identical conditions, where additional fat and milk fat globules are removed. Once again, the upper and lower layers are discarded, and the remaining supernatant undergoes Step 3 centrifugation, conducted at 5000 × *g* for 30 min at 4°C, to further separate fat and cell debris. Finally, the clarified middle phase is processed in Step 4, where centrifugation at 10,000 × *g* for 30 min at 4°C removes residual fat, fat globules, large vesicles and protein aggregates. EVs remain in the skimmed milk fraction, which can be collected for further isolation. Figure S1 shows the ATR-FTIR spectra of raw HM sample (red) and skimmed HM (black) obtained after preprocessing. The disappearance of the absorption band at 1750 cm^{-1}, primarily associated with ester groups in phospholipids, triglycerides and cholesterol esters, indicates the effective removal of lipid components in the skimmed HM sample. Moreover, the reduced intensity of the CH_2 stretching bands from lipid acyl groups at 2921 and 2851 cm^{-1} further indicates the depletion of lipids during the skimming process.

Casein removal is another crucial step in the extraction of pure EVs from HM. Several methods have been reported, yet acidic treatments have emerged as highly effective in quantitatively isolating EVs. Although some studies suggest that acidic treatments may cause minor alterations to the outer lipid bilayer, the internal structure of EVs remains intact (Rahman et al. 2019). This structural stability allows them to withstand acidic conditions, such as those encountered in the stomach, and retain their antiinflammatory properties upon reaching the intestine (Yamauchi et al. 2019). To achieve an effective casein removal while preserving EV integrity, four different precipitation methods were tested. Western blot analysis (Figure 3) showed that HCl treatment resulted in the lowest β-casein levels. This result was further confirmed by ATR-FTIR analysis, which showed a 29% reduction in total protein, as indicated by the decreased area of the Amide I band (1724–1591 cm^{-1}). Given that casein constitutes 20%–50% of total HM protein throughout lactation, with an average of 35% (Lönnerdal 2003), the observed protein reduction

27682811, 2026, 1, Downloaded from https://isevjournals.onlinelibrary.wiley.com/doi/10.1002/jex2.70110 by Spanish Cochrane National Provision (Ministerio de Sanidad), Wiley Online Library on [11/03/2026]. See the Terms and Conditions (https://onlinelibrary.wiley.com/terms-and-conditions) on Wiley Online Library for rules of use; OA articles are governed by the applicable Creative Commons License

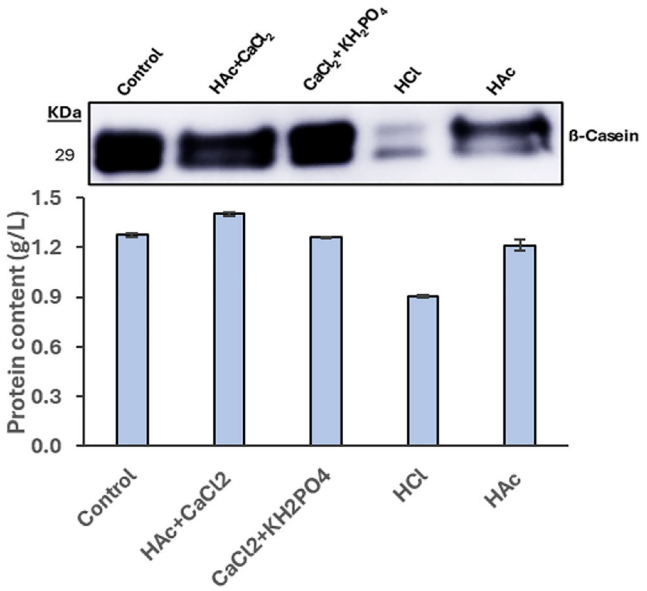


FIGURE 3 | Evaluation of different beta-casein removal approaches. Beta-casein bands from Western blot analysis (top) and total protein content determined by ATR-FTIR (bottom). Control = skimmed HM. Error bars indicate standard deviation ($N = 3$). ATR-FTIR, attenuated total reflectance–Fourier transform infrared; $CaCl_2$, calcium chloride; HAc, acetic acid; HCl, hydrochloric acid; KH_2PO_4, potassium dihydrogen phosphate.

aligns well with the expected casein depletion, supporting the reliability and effectiveness of HCl precipitation. These findings are consistent with prior reports identifying acidification (to pH ~4.3) as an efficient strategy for casein removal that improves downstream EV isolation, with only minimal effects on vesicle morphology (Van Herwijnen et al. 2016; Cetinkaya et al. 2024).

Skimmed and acidified HM samples were further subjected to SEC for the isolation of HMEVs. TEM imaging of Fractions 1–4 confirmed the presence of isolated EVs, exhibiting the characteristic spherical morphology (Webber and Clayton 2013) (see Figure S2, top). The typical 'cup-shaped' morphology commonly described for EVs was less evident in recorded TEM images. This observation can be attributed to the acidification step used during casein micelle removal, which has been shown to slightly alter vesicle membrane structure and reduce the characteristic concavity in TEM micrographs, occasionally decreasing image clarity and contrast. This phenomenon has been reported in HMEVs processed using acid-based casein precipitation (Cetinkaya et al. 2024). Despite these mild morphological alterations, particle size distribution, concentration and EV marker profiles remained within the expected ranges for HMEVs. In contrast, TEM images of Fractions 5–7 (see Figure S2, bottom) revealed protein aggregates lacking EV morphologies. TRPS measurements (Figure 4, bottom) showed EV concentrations ranging from $(2.8 \pm 0.8) \times 10^{10}$ to $(7 \pm 2) \times 10^{9}$ particles/mL in Fractions 1–4. Particle size analysis of nanoparticles in suspension, without additional sample preparation, indicated mode sizes from 122 nm in Fraction 1 to 107 nm in Fraction 4. Additionally, Western blot analysis of EV-specific biomarkers CD81 and Alix (Figure 4, top) confirmed the presence of EVs in Fractions 1–3, while Fraction 4 tested negative. This absence may be attributed to the lower concentration of EVs, as evidenced by TRPS measurements.

3.2 | Optimisation of Sample Collection, Handling and Storage

Sample collection, handling and storage are critical steps in clinical studies and must be carefully considered during workflow optimisation. To evaluate their impact, three different procedures (HM-DP, HMS1 and HMS2) were compared alongside the previously developed dUC-based (HMS2-dUC), as summarised in Figure 1. Western blot analysis (Figure 5, bottom) confirmed the presence of EVs by detecting Alix while showing the absence of β-casein across all procedures. EV concentrations measured by TRPS (see Figure 5, top) revealed similar yields for HM-DP and HMS1, whereas significantly lower concentrations were observed for HMS2 and HMS2-dUC. Notably, the Alix signal appeared comparatively stronger in the skimmed and frozen sample (HMS2) than in the unskimmed one (HMS1), despite the higher particle counts detected in HMS1. This observation suggests that a proportion of the additional particles in HMS1 may not correspond to Alix-positive vesicles. Furthermore, HMS2-dUC yielded lower EV concentrations than all SEC-based procedures, confirming the higher efficiency of SEC for EV isolation.

Tetraspanin colocalisation analysis was performed to assess the impact of storage and processing conditions on the membrane protein composition of HMEVs. Principal component analysis (PCA) of tetraspanin colocalisation data (Figure S3) showed a clear separation between freshly processed milk (HM-DP) and samples obtained from frozen conditions (HMS1, HMS2 and HMS2-dUC). This distinction along PC1 primarily reflects the effect of sample handling and processing steps, including freezing and thawing cycles. According to the loadings plot, HM-DP samples exhibited a stronger contribution of CD81-positive particles, HMS2 and HMS2-dUC were enriched in CD9-positive vesicles, and HMS1 displayed a higher proportion of CD63-positive vesicles. These findings indicate that storage conditions, freeze–thaw cycles and processing sequence can influence the relative distribution of tetraspanin subpopulations in HMEV isolates (see Figure S3).

The presence of potential coisolated compounds was assessed by ATR-FTIR spectroscopy (Figure 6a). Results revealed that HMS1 and HMS2-dUC showed intense bands across the fingerprint region indicating coisolated nucleic acids, proteins and lipids (Ramos-Garcia et al. 2021). The intense absorption in the Amide I region observed in samples prepared following HMS1, indicated a higher concentration of coisolated proteins, likely resulting from protein release during freezing-induced cell lysis. In contrast, HMS2-dUC showed a higher lipid coisolation, characterised by a pronounced signal intensity in the CH-stretching region (2800–3000 cm^{-1}). Moreover, HMS2-dUC also showed a characteristic Amide I/II profile indicative of protein aggregation caused by high shear forces during UC (Webber and Clayton 2013), which was not observed with the other methods due to protein removal (i.e., acidification and SEC) steps.

The purity of HMEV isolates was further assessed by calculating particle-to-protein concentration ratio (Figure 6b) (Webber and

27682811, 2026, 1, Downloaded from https://isevjournals.onlinelibrary.wiley.com/doi/10.1002/jex2.70110 by Spanish Cochrane National Provision (Ministerio de Sanidad), Wiley Online Library on [11/03/2026]. See the Terms and Conditions (https://onlinelibrary.wiley.com/terms-and-conditions) on Wiley Online Library for rules of use; OA articles are governed by the applicable Creative Commons License

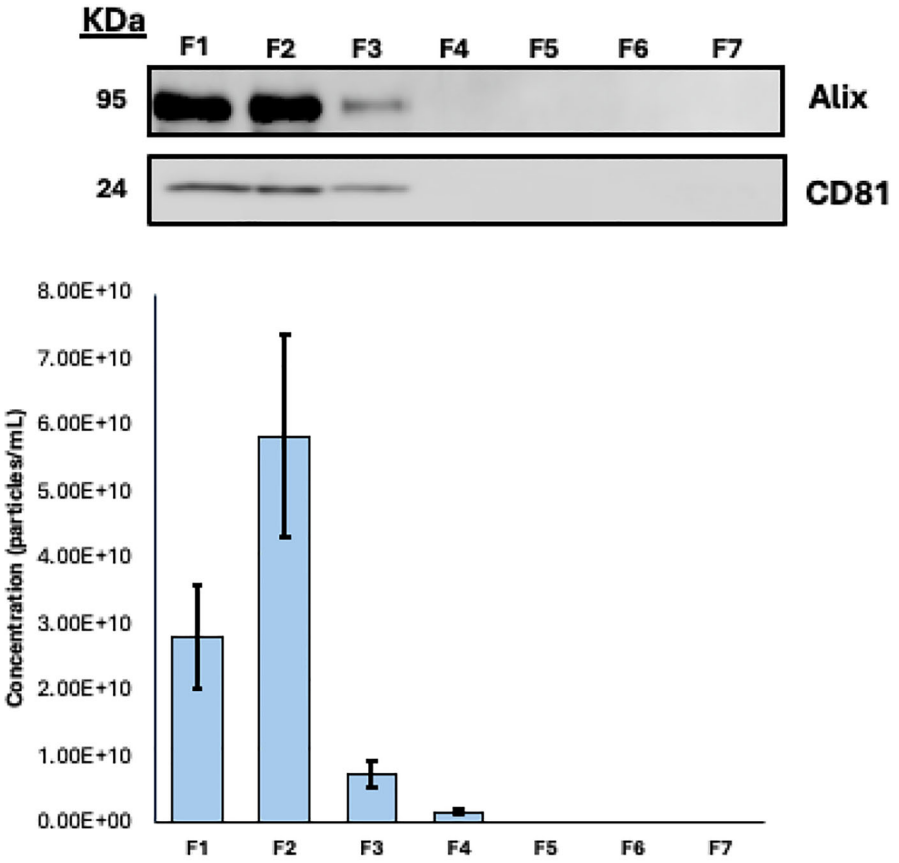


FIGURE 4 | Characterisation of SEC Fractions 1–7. Western blot assay confirming the presence of EVs (top) and TRPS particle count (bottom). *Note:* Error bars indicate the standard deviation calculated from three independent TRPS replicate measurements conducted under identical conditions. EV, extracellular vesicle; SEC, size-exclusion chromatography; TRPS, tunable resistive pulse sensing.

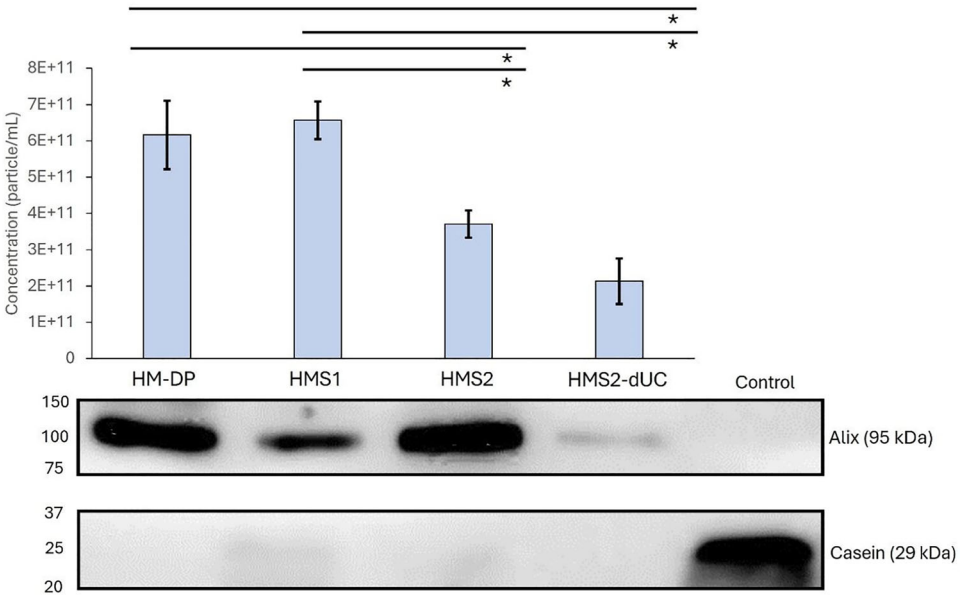


FIGURE 5 | (Top) EV concentrations for the four tested processing and storage procedures. *Note:* Each condition was evaluated using two independent replicates; *one-way ANOVA with Tukey's post hoc test was used for identifying significant differences (i.e., p values <0.05); EV concentrations were normalised to HM volume. (Bottom) Western blot analysis for the method (from HM-DP to HMS2-dUC) and casein positive control. DP, direct processing; dUC, differential ultracentrifugation; EV, extracellular vesicle; HM, human milk; HMS, HM storage.

27682811, 2026, 1, Downloaded from https://isevjournals.onlinelibrary.wiley.com/doi/10.1002/jex2.70110 by Spanish Cochrane National Provision (Ministerio de Sanidad), Wiley Online Library on [11/03/2026]. See the Terms and Conditions (https://onlinelibrary.wiley.com/terms-and-conditions) on Wiley Online Library for rules of use; OA articles are governed by the applicable Creative Commons License

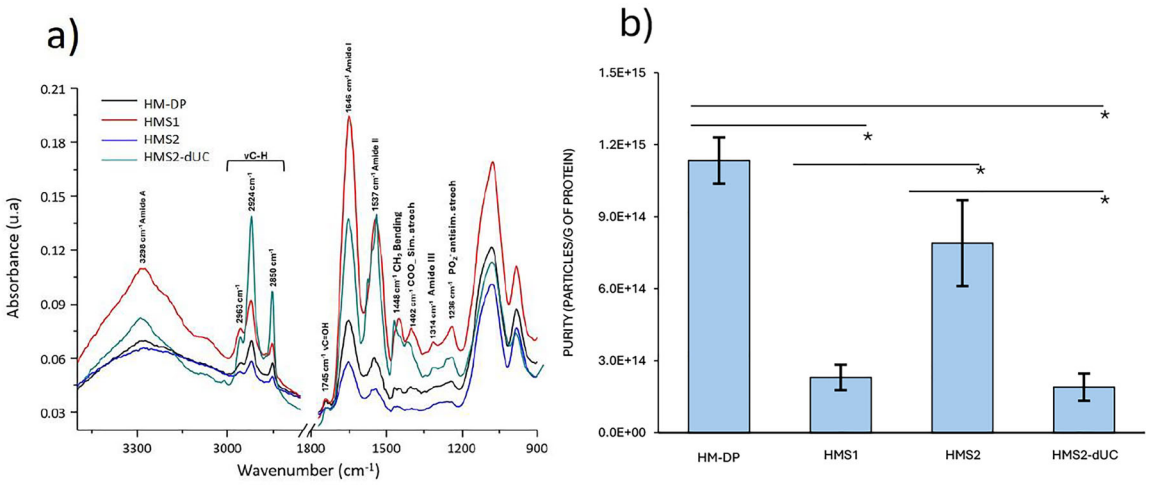


FIGURE 6 | (a) ATR-FTIR spectra of HMEVs from HM-DP to HMS2-dUC, using a spectrum of PBS as a background. (b) Purity of isolated EVs for the four tested processing and storage procedures. *Note:* Two independent replicates were tested in each condition. *One-way ANOVA with Tukey's post hoc test was used to identify significant differences (i.e., p values <0.05). ATR-FTIR, attenuated total reflectance–Fourier transform infrared; DP, direct processing; dUC, differential ultracentrifugation; HM, human milk; HMS, HM storage.

Clayton 2013). From results depicted in Figure 6b, the use of fresh HM (HM-DP) provided the highest particle-to-protein ratios, followed by method HMS2. When immediate processing is not feasible, skimmed and frozen HM processed with SEC (HMS2) offers a viable alternative, balancing purity and practicality, whereas methods HMS1 and HMS2-dUC compromise EV quality due to significant protein and/or lipid contamination.

These observations are consistent with previous reports showing that sample freezing and subsequent freeze–thaw cycles can compromise EV integrity, promoting cell disruption and the release of nonvesicular material, which may artificially increase particle counts and affect downstream analyses (Ahmadian et al. 2024; Gelibter et al. 2022). Accordingly, several studies have emphasised the importance of skimming or removing the cream layer and cellular debris before freezing to prevent coisolation of cellular fragments and milk fat globule membranes during later EV isolation (Van Herwijnen et al. 2016). In agreement with these findings, our results indicate that preskimming before storage (HMS2) preserves EV-associated markers and reduces nonvesicular contaminants compared to unskimmed frozen samples (HMS1). Altogether, these results reinforce that proper preanalytical handling, particularly skimming prior to freezing, is essential to minimise freeze–thaw-induced artefacts and ensure reproducible recovery of HMEVs.

3.3 | Maximising Oxylipin Recovery From HMEV Isolates

To determine the oxylipin content in EVs, a lysis step was performed to extract them from the vesicle core. A pool of HM was employed. MeOH and ACN were tested individually and in combination with freeze/thaw cycles in liquid nitrogen. As shown in Figure S4, the inclusion of freeze/thaw cycles in liquid nitrogen resulted in a significant reduction in fluorescence intensity, indicating more efficient vesicle disruption. Based on its compatibility with the subsequent oxylipin extraction process, MeOH was selected as the optimal lysis solvent.

Oxylipin extraction and preconcentration were performed using SPE before UPLC-MS/MS analysis. Two SPE stationary phases, that is, Oasis HLB and Oasis MAX, were tested in triplicate to assess the recovery of 23 target oxylipins. Figure S5 summarises the recoveries and precision observed for each analyte across three independent replicates. The Oasis HLB column outperformed Oasis MAX, achieving optimal recoveries (80%–120%) for 87% of oxylipins, with an average RSD of 6%. In contrast, the Oasis MAX plate yielded acceptable (80%–120%) recoveries for 73% of tested oxylipins but exhibited significantly higher variability (average RSD of 33%). Based on these results, the Oasis HLB column was selected for further analyses. The method's analytical performance metrics are detailed in Table 1. Additionally, the effect of adding the antioxidant BHT was evaluated. Although BHT had previously been added only to the extracts, in this study it was also incorporated into preprocessed skimmed HM samples before storage to assess its impact on oxylipin stability and recovery. As shown in Figure S6, inclusion of BHT markedly increased the number of oxylipins detected above the limit of quantification (LOQ) and improved overall oxylipin concentrations compared to samples processed without antioxidant protection. Notably, the levels of 12,13-DiHOME, 9,10-DiHOME, 5,6-EET, 14,15-EET, 11,12-EET and 8,9-EET were substantially higher in the presence of BHT, reflecting enhanced analyte preservation. These findings highlight the beneficial role of antioxidants in improving oxylipin detection and stability during sample storage and extraction. Importantly, BHT improved overall oxylipin preservation by preventing oxidative degradation throughout handling and processing but did not selectively enhance the recovery of the eight oxylipins, as shown in Figure S6. The observed increases likely reflect a global stabilisation effect rather than compound-specific enrichment.

27682811, 2026, 1, Downloaded from https://isevjournals.onlinelibrary.wiley.com/doi/10.1002/jex2.70110 by Spanish Cochrane National Provision (Ministerio de Sanidad), Wiley Online Library on [11/03/2026]. See the Terms and Conditions (https://onlinelibrary.wiley.com/terms-and-conditions) on Wiley Online Library for rules of use; OA articles are governed by the applicable Creative Commons License

TABLE 1 | Figures of merit and detection rates of the UPLC-MS/MS profiling of oxylipinsin HMEVs.

Analyte	R^2	Calibration range (nM)	RT (min)	LOD (nM)	LOQ (nM)	LLOQ in EVs isolate (nM)	LLOQ in HM (nM)	% Detected	% Quantified
12,13-DiHOME	0.9943	0.11–225	4.56	0.033	0.11	0.028	0.0011	100	100
9,10-DiHOME	0.9937	0.44–225	4.7	0.132	0.44	0.110	0.0044	100	100
18-HEPE	0.9903	0.22–225	5.11	0.066	0.22	0.055	0.0022	0	0
17,18-DiHETE	0.9965	0.11–225	4.34	0.033	0.11	0.028	0.0011	0	0
8(S) 15(S)-DiHETE	0.9939	0.44–225	4.46	0.132	0.44	0.110	0.0044	0	0
14,15-DiHETE	0.9961	0.22–225	4.46	0.066	0.22	0.055	0.0022	0	0
14-HDHA | 14-HDoHE	0.9921	0.22–225	5.73	0.066	0.22	0.055	0.0022	10	10
17-HDHA | 17-HDoHE	0.9960	0.44–225	5.63	0.132	0.44	0.110	0.0044	0	0
19,20-DiHDPA	0.9960	0.22–225	4.8	0.066	0.22	0.055	0.0022	0	0
PGE_2	0.9974	0.22–225	3.2	0.066	0.22	0.055	0.0022	0	0
Maresin-2	0.9949	0.11–225	4.69	0.033	0.11	0.028	0.0011	0	0
PDX	0.9908	0.22–225	4.34	0.066	0.22	0.055	0.0022	0	0
TXB_2	0.9944	0.44–226	2.89	0.132	0.44	0.110	0.0044	0	0
$PGF_{2\alpha}$	0.9966	0.22–225	3.14	0.066	0.22	0.055	0.0022	0	0
LTB_4	0.9947	0.11–225	4.5	0.033	0.11	0.028	0.0011	0	0
5,6-EET	0.9922	0.44–225	6.42	0.132	0.44	0.110	0.0044	10	0
14,15-EET	0.9927	0.44–225	6.1	0.132	0.44	0.110	0.0044	10	10
11,12-EET	0.9925	0.11–225	6.27	0.066	0.22	0.028	0.0011	50	30
8,9-EET	0.9969	0.11–225	6.34	0.066	0.22	0.028	0.0011	30	10
8,9-DiHET	0.9948	0.11–225	5.16	0.033	0.11	0.028	0.0011	0	0
14,15-DiHET	0.9962	0.11–225	4.81	0.033	0.11	0.028	0.0011	20	0
5,6-DiHET	0.9925	0.22–225	5.38	0.066	0.22	0.055	0.0022	0	0
11,12-DiHET	0.9925	0.22–225	4.99	0.066	0.22	0.055	0.0022	0	0

Note: The lower limits of quantification (LLOQs) were defined as the analyte concentration with <20% imprecision and deviation from the true value, accounting for the preconcentration factor applied during sample processing. The limit of detection (LOD) was set at 3/10*LOQ. '% Detected' and '% Quantified' indicate the percentage of oxylipins detected and quantified across the 10 analysed samples.

27682811, 2026, 1, Downloaded from https://isevjournals.onlinelibrary.wiley.com/doi/10.1002/jex2.70110 by Spanish Cochrane National Provision (Ministerio de Sanidad), Wiley Online Library on [11/03/2026]. See the Terms and Conditions (https://onlinelibrary.wiley.com/terms-and-conditions) on Wiley Online Library for rules of use; OA articles are governed by the applicable Creative Commons License

3.4 | Final Isolation Protocol of HMEVs Applied to HM Samples

The developed EV isolation workflow was applied to 10 HM samples (see Section 2.2). Metadata are available in Table S3. The final protocol selected consisted in the following steps: First, 7 mL of HM was centrifuged at 3000 × *g* for 10 min at RT. The supernatant was supplemented with 0.01% BHT and stored at −80°C. On the day of isolation, it was centrifuged at 5000 and 10,000 × *g* at 4°C, diluted 1:1 with Milli-Q water, adjusted to pH 4.3 with 1 M HCl and centrifuged again at 5100 × *g* for 20 min at 4°C. The resulting supernatant was filtered (0.45 μm), processed by SEC, and the eluate ultracentrifuged at 175,000 × *g* for 2 h at 4°C. The final pellet was resuspended in PBS with 0.01% BHT and stored at −80°C until oxylipin analysis. Isolated HMEVs were characterised in terms of yield, particle size, protein content, purity and membrane proteins.

The number of EVs in HM isolates yielded concentration values ranging from 9×10^9 to 4×10^{10} EVs/mL (RSD = 47%, median = 2×10^{10} EVs/mL) and mode size range from 106 to 124 nm (RSD = 6%, median = 113 nm) with all samples (Figure S7), showing a similar size distribution profile characterised by a single maximum. Total protein contents determined by ATR-FTIR spectroscopy ranged from 1×10^3 to 4×10^3 μg/mL (RSD = 49%, median = 3×10^3 μg/mL). The purity of the isolated EVs was evaluated using the particle-to-protein ratio, which ranged from 1×10^{14} to 3×10^{14} particles/g protein (RSD = 33%, median = 2×10^{14} particles/g of protein). Comparing the characterisation results with the clinical variables summarised in Table S2, we observed a marked decrease in HMEV concentration with increasing maternal age (Pearson $r = -0.90$, $p = 0.0006$; Figure S8). Other variables, including gestational age ($r = -0.33$, $p = 0.36$), postnatal age ($r \approx -0.18$, $p = 0.63$), type of delivery (Mann–Whitney $U = 2.0$, $p = 0.18$) and term status ($U = 0.0$, $p = 0.20$), showed mild but nonsignificant trends, likely due to the limited cohort size. These tendencies warrant further investigation in larger studies. The negative association between HMEV concentration and maternal age may reflect age-related alterations in mammary gland physiology. Mammary tissue ageing is characterised by a reduction in stromal cell abundance, which compromises paracrine signalling and the overall secretory capacity of the gland (Neville et al. 2001). Likewise, the decline in HMEVs could arise from diminished secretory activity of alveolar cells (lactocytes) (Li et al. 2020), age-associated remodelling of the cytoskeleton and plasma membrane (Schedin and Keely 2011), and dysregulation of hormonal control and intercellular communication pathways.

Tetraspanin colocalisation analysis was performed, with Figure 7 displaying images from a representative sample. The large number of EVs isolated from HM samples is clearly visible across all three tetraspanin capture antibodies against CD9 (Figure 7a), CD81 (Figure 7b) and CD63 (Figure 7c), providing a marked contrast to the MIgG (Figure 7d), the negative control. PCA revealed two distinct sample groups (Figure 8a), separated along PC1. According to the loadings plot (Figure 8b), this separation was mainly driven by differences in the relative abundance of tetraspanin-positive subpopulations (CD9, CD63 and CD81). Samples with negative PC1 values were associated with higher proportions of single-positive vesicles, whereas those with positive PC1 values showed a greater contribution of double- and triple-positive subpopulations. A colour scale representing particle concentration measured by TRPS was overlaid in Figure 8a to visualise whether the PCA grouping coincided with differences in total particle counts. Although samples with higher particle concentrations tended to cluster at positive PC1 values, the main drivers of separation correspond to the tetraspanin distribution patterns identified in the loading plot.

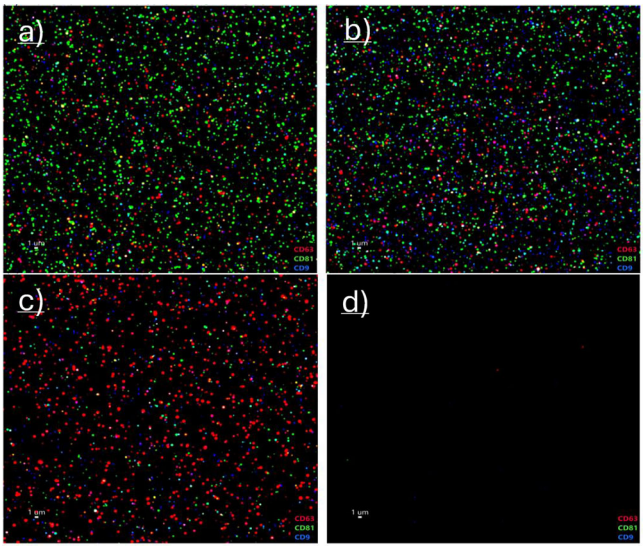


FIGURE 7 | CD9, CD81 and CD63 colocalisation in EVs from a representative HM sample. EV, extracellular vesicle; HM, human milk.

3.5 | Quantitative Analysis of HMEVs Oxylipin Profile

After isolation and thorough characterisation, oxylipins were detected using UPLC MS/MS (see Table S4). Figure 9a presents the concentration levels of oxylipins in HMEVs. Out of the 23 oxylipins, the method successfully detected eight compounds (35%). Among these, 12,13-DiHOME and 9,10-DiHOME were consistently detected and quantified in all samples (100%), underscoring their ubiquity and potential relevance (see Table 1). In contrast, other oxylipins exhibited lower detection/quantification frequencies ranging between 10% and 50%. Importantly, this is the first time that arachidonic acid-derived EETs have been detected in HMEVs. These molecules are well known for their potent antiinflammatory and neuroprotective properties (Spector and Norris 2007; Wang et al. 2018; Panigrahy et al. 2013). Their antiinflammatory effects are primarily mediated through the inhibition of proinflammatory pathways, such as NF-κB signalling, and the activation of PPAR-γ, a key regulator of fatty acid metabolism and inflammation. The presence of EETs in HMEVs suggests a potential mechanism by which these vesicles mitigate inflammatory conditions, enhance endothelial function, promote vasodilation and support tissue repair (Macêdo et al. 2022). Additionally, the presence of 12,13-DiHOME and 9,10-DiHOME in all 10 studied HM samples reaffirms their biological relevance. Once thought to be proinflammatory (Hildreth et al. 2020), these molecules are now recognised for their inverse association with the body mass index and their beneficial role in metabolism by stimulating calcium influx in adipocytes, making them potential therapeutic targets for metabolic disorders (Dreyfuss et al. 2024; Lynes et al.

27682811, 2026, 1, Downloaded from https://isevjournals.onlinelibrary.wiley.com/doi/10.1002/jex2.70110 by Spanish Cochrane National Provision (Ministerio de Sanidad), Wiley Online Library on [11/03/2026]. See the Terms and Conditions (https://onlinelibrary.wiley.com/terms-and-conditions) on Wiley Online Library for rules of use; OA articles are governed by the applicable Creative Commons License

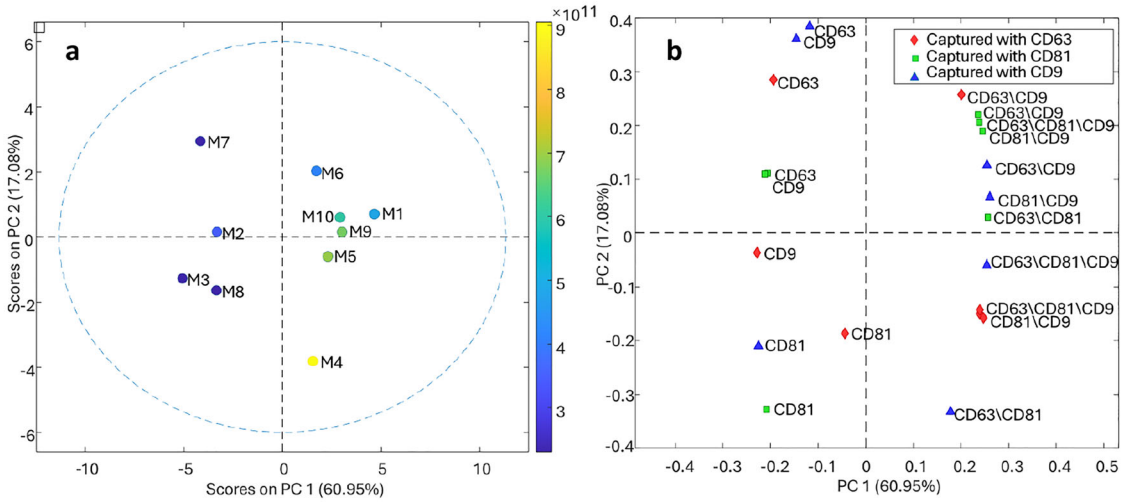


FIGURE 8 | Tetraspanin colocalisation analysis for HMEVs isolates. (a) PCA scores plots. *Note:* Colour scale indicates particle count in particles/mL by TRPS. (b) PCA loadings plots. HMEVs, human milk extracellular vesicle; PCA, principal component analysis; TRPS, tunable resistive pulse sensing.

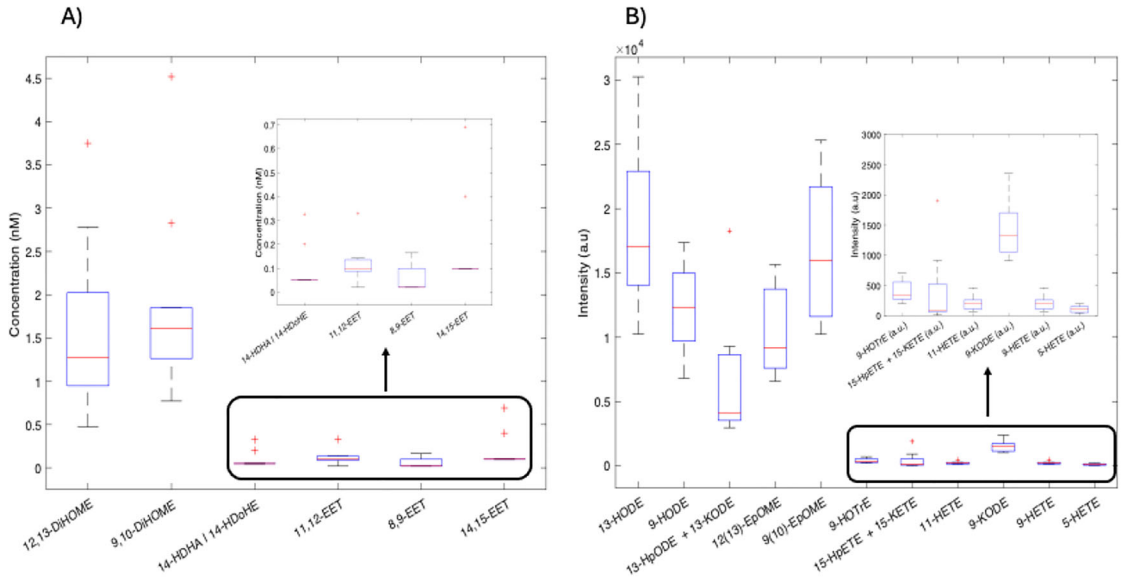


FIGURE 9 | The oxylipin profile of HMEVs. (a) Quantified oxylipins in milk-derived EVs using the UPLC-MS/MS method. (b) Semiquantitative detection of oxylipins in milk-derived EVs using the UPLC-MS/MS method. EV, extracellular vesicle; HMEVs, human milk extracellular vesicles; UPLC-MS/MS, ultra-performance liquid chromatography–tandem mass spectrometry.

2017; Czosnykowska-Łukacka et al. 2018). The combination of DiHOMEs with antiinflammatory EETs underscores the diverse bioactive potential of HMEVs, positioning them as promising tools for therapeutic interventions targeting inflammation and tissue repair. However, some oxylipins, such as 17-HDHA and 12-HpETE, that had been reported to be present in HMEVs earlier (Albiach-Delgado et al. 2024), were not detected in this study, highlighting variations due to potential changes in oxylipin concentration among biological samples, or effects of preservation conditions and isolation methods.

Furthermore, Figure 9b showcases the results obtained through semiquantitative oxylipin screening, highlighting relative intensities of putatively detected oxylipins. In comparison with a previous study reporting oxylipin abundance values of 10^2 (Albiach-Delgado et al. 2024), the current analysis demonstrated a substantial increase, with oxylipin signal intensities approximately 100-fold higher levels. This difference may be attributed to changes in the workflow and the higher postnatal age of the breastfed infants included in this study, with a median of 375 days compared to 25 days in the previous study. As lipid secretion has been shown to increase with the infant's age (Imig 2012), this could lead to changes in the composition of polyunsaturated fatty acids and their oxylipin derivatives.

4 | Conclusions

In this study, we developed and optimised a comprehensive workflow for the isolation and characterisation of HMEVs,

27682811, 2026, 1, Downloaded from https://isevjournals.onlinelibrary.wiley.com/doi/10.1002/jex2.70110 by Spanish Cochrane National Provision (Ministerio de Sanidad), Wiley Online Library on [11/03/2026]. See the Terms and Conditions (https://onlinelibrary.wiley.com/terms-and-conditions) on Wiley Online Library for rules of use; OA articles are governed by the applicable Creative Commons License

emphasising the impact of procedural and analytical steps and their importance to ensure the high quality of retrieved oxylipin profiles. A systematic sequence of several critical methodological refinements was considered, including optimised milk preprocessing, stringent storage conditions and effective fat and casein removal, with the combination of SEC and UC proving superior to dUC in terms of vesicle recovery, purity and structural integrity. The optimised SEC + UC workflow further demonstrated a substantial improvement in EV yield and practicality compared with ultracentrifugation alone. When normalised to the same starting volume, TRPS analysis showed that SEC + UC achieved approximately threefold higher vesicle concentration, while requiring only 7 mL of milk compared to the 25 mL needed for UC. These results highlight not only the higher recovery efficiency of the combined approach but also its greater scalability and suitability for studies where HM availability is limited. The integration of SEC and UC thus provides a reproducible, high-yield workflow adaptable to both small- and large-scale research settings. A wide range of characterisation tools were employed to confirm vesicle identity and quality, including Western blot for protein marker detection, TRPS for size and concentration analysis, and ATR-FTIR spectroscopy to assess the molecular composition of the vesicles. This methodological framework was validated using 10 HM samples from donors, confirming reproducibility and reliability across independent preparations. As a complementary analysis, targeted oxylipin profiling by UPLC-MS/MS enabled the detection of eight oxylipins, including 12,13-DiHOME, 9,10-DiHOME, 14-HDHA, 14,15-DiHET and several EETs (5,6-EET, 11,12-EET, 8,9-EET and 14,15-EET), which, may suggest a potential role for HMEVs in modulating inflammatory responses, in agreement with previous studies (Morisseau and Hammock 2013; Serhan and Levy 2018). Beyond the identification of bioactive lipid mediators, the core contribution of this study lies in the establishment of a reproducible and scalable workflow for the procedural isolation and molecular characterisation of HMEVs. This lays the groundwork for future investigations into their biological function and therapeutic potential in inflammatory, metabolic and neonatal health contexts such as NEC.

Author Contributions

Jose Luis Moreno-casillas: writing – original draft, writing – review and editing, methodology, investigation, formal analysis, data curation. **Laura Ripoll-seguer**: data curation, writing – original draft, writing – review and editing, methodology, investigation, formal analysis. **Isabel Ten-doménech**: writing – review and editing, visualisation, supervision. **Marta Gómez-ferrer**: supervision, writing – review and editing, methodology, investigation. **Pilar Sepúlveda**: writing – review and editing, supervision, resources, project administration, funding acquisition, conceptualisation. **Abel Albiach-delgado**: writing – review and editing, methodology, formal analysis, data curation. **Juan Daniel Sanjuan-herráez**: formal analysis, writing – review and editing. **María Gormaz**: writing – review and editing, supervision. **David Pérez-guaita**: writing – review and editing, validation, supervision, resources, project administration, methodology, funding acquisition, conceptualisation. **Bernhard Lendl**: writing – review and editing, resources, funding acquisition. **María Cernada**: writing – review and editing, supervision, resources, conceptualisation. **Guillermo Quintás**: writing – review and editing, visualisation, validation, supervision, resources, software, project administration, funding acquisition, formal analysis, conceptualisation. **Julia Kuligowski**: writing – review and editing, visualisation, validation, supervision, software, resources, project administration, funding acquisition, conceptualisation, formal analysis.

Funding

This work was supported by the *Instituto de Salud Carlos III* (ISCIII), Spain, and co-funded by the European Union under grant numbers FI21/00193, CD22/00081, and PI23/00202; the *Conselleria d'Innovació, Universitats, Ciència i Societat Digital*, *Generalitat Valenciana*, Spain, under grant numbers CIAICO/2022/233 and CPI-22-674; and *Conselleria d'Educació, Cultura, Universitats i Ocupació*, *Generalitat Valenciana*, Spain and *Fons Social Europeu Plus* (FSE+).

Ethics Statement

The study protocol was approved by the Ethics Committee for Biomedical Research of the Health Research Institute La Fe (Valencia, Spain) with approval number #2022-922-1. All procedures were carried out in compliance with the Declaration of Helsinki.

Consent

All volunteers gave their informed consent for inclusion before being enrolled in the study.

Conflicts of Interest

The authors declare no conflicts of interest.

Data Availability Statement

Raw data from the characterisation of HMEVs including TRPS size distribution and count, ATR-FTIR spectra and ExoView surface protein colocalisation are available at the Zenodo repository under https://doi.org/10.5281/zenodo.16029124.

References

Ahmadian, S., N. Jafari, A. Tamadon, A. Ghaffarzadeh, R. Rahbarghazi, and M. Mahdipour. 2024. "Different Storage and Freezing Protocols for Extracellular Vesicles: A Systematic Review." *Stem Cell Research & Therapy* 15, no. 1: 453. https://doi.org/10.1186/s13287-024-04005-7.

Albiach-Delgado, A., J. L. Moreno-Casillas, I. Ten-Doménech, et al. 2024. "Oxylipin Profile of Human Milk and Human Milk-Derived Extracellular Vesicles." *Analytica Chimica Acta* 1313: 342759.

Anaya, K., N. Sus, C. Gadelha, and J. Frank. 2019. "Development and Validation of a Rapid Reversed-Phase Liquid Chromatography Method for CnAMP1 Peptide Quantification in Human Intestinal Cell Lines." *Amino Acids* 51, no. 3: 407–418. https://doi.org/10.1007/s00726-018-2675-7.

Benedikter, B. J., F. G. Bouwman, T. Vajen, et al. 2017. "Ultrafiltration Combined With Size Exclusion Chromatography Efficiently Isolates Extracellular Vesicles From Cell Culture Media for Compositional and Functional Studies." *Scientific Reports* 7, no. 1: 15297. https://doi.org/10.1038/s41598-017-15717-7.

Burge, K., F. Vieira, J. Eckert, and H. Chaaban. 2021. "Lipid Composition, Digestion, and Absorption Differences Among Neonatal Feeding Strategies: Potential Implications for Intestinal Inflammation in Preterm Infants." *Nutrients* 13, no. 2: 550. https://doi.org/10.3390/nu13020550.

Cetinkaya, H., S. Kongsomros, L. Nommsen-Rivers, A. L. Morrow, and S. Chutipongtanate. 2024. "Which Casein Micelle Removal Method Is Suitable for Studies of Human Milk Extracellular Vesicles? A Systematic Comparison of Four Different Treatments for Casein Depletion Before Extracellular Vesicle Isolation From Human Milk." *Extracellular Vesicles and Circulating Nucleic Acids* 5, no. 2: 221–232. https://doi.org/10.20517/evcna.2024.02.

Chen, W., X. Chen, Y. Qian, et al. 2021. "Lipidomic Profiling of Human Milk Derived Exosomes and Their Emerging Roles in the Prevention of

27682811, 2026, 1, Downloaded from https://isevjournals.onlinelibrary.wiley.com/doi/10.1002/jex2.70110 by Spanish Cochrane National Provision (Ministerio de Sanidad), Wiley Online Library on [11/03/2026]. See the Terms and Conditions (https://onlinelibrary.wiley.com/terms-and-conditions) on Wiley Online Library for rules of use; OA articles are governed by the applicable Creative Commons License

Necrotizing Enterocolitis." *Molecular Nutrition & Food Research* 65, no. 10: 2000845. https://doi.org/10.1002/mnfr.202000845.

Chutipongtanate, S., A. L. Morrow, and D. S. Newburg. 2022. "Human Milk Extracellular Vesicles: A Biological System With Clinical Implications." *Cells* 11, no. 15: 2345. https://doi.org/10.3390/cells11152345.

Czosnykowska-Łukacka, M., B. Królak-Olejnik, and M. Orczyk-Pawiłowicz. 2018. "Breast Milk Macronutrient Components in Prolonged Lactation." *Nutrients* 10, no. 12: 1893. https://doi.org/10.3390/nu10121893.

Dreyfuss, J. M., V. Djordjilović, H. Pan, et al. 2024. "ScreenDMT Reveals DiHOMEs Are Replicably Inversely Associated With BMI and Stimulate Adipocyte Calcium Influx." *Communications Biology* 7, no. 1: 996. https://doi.org/10.1038/s42003-024-06646-z.

Gelibter, S., G. Marostica, A. Mandelli, et al. 2022. "The Impact of Storage on Extracellular Vesicles: A Systematic Study." *Journal of Extracellular Vesicles* 11, no. 2: e12162. https://doi.org/10.1002/jev2.12162.

Gómez-Ferrer, M., E. Amaro-Prellezo, A. Albiach-Delgado, I. Ten-Domenech, J. Kuligowski, and P. Sepúlveda. 2023. "Identification of Omega-3 Oxylipins in Human Milk-Derived Extracellular Vesicles With Pro-Resolutive Actions in Gastrointestinal Inflammation." *Frontiers in Immunology* 14: 1293737. https://doi.org/10.3389/fimmu.2023.1293737.

Grätz, C., M. Schuster, F. Brandes, et al. 2024. "A Pipeline for the Development and Analysis of Extracellular Vesicle-Based Transcriptomic Biomarkers in Molecular Diagnostics." *Molecular Aspects of Medicine* 97: 101269. https://doi.org/10.1016/j.mam.2024.101269.

Guerreiro, E. M., B. Vestad, L. A. Steffensen, et al. 2018. "Efficient Extracellular Vesicle Isolation by Combining Cell Media Modifications, Ultrafiltration, and Size-Exclusion Chromatography." *PLoS ONE* 13, no. 9: e0204276. https://doi.org/10.1371/journal.pone.0204276.

Herwijnen, M. J. C. V., T. A. P. Driedonks, B. L. Snoek, et al. 2018. "Abundantly Present miRNAs in Milk-Derived Extracellular Vesicles Are Conserved Between Mammals." *Frontiers in Nutrition* 5: 81. https://doi.org/10.3389/fnut.2018.00081.

Hildreth, K., S. D. Kodani, B. D. Hammock, and L. Zhao. 2020. "Cytochrome P450-Derived Linoleic Acid Metabolites EpOMEs and DiHOMEs: A Review of Recent Studies." *Journal of Nutritional Biochemistry* 86: 108484. https://doi.org/10.1016/j.jnutbio.2020.108484.

Hu, Y., J. Thaler, and R. Nieuwland. 2021. "Extracellular Vesicles in Human Milk." *Pharmaceuticals* 14, no. 10.

Imig, J. D. 2012. "Epoxides and Soluble Epoxide Hydrolase in Cardiovascular Physiology." *Physiological Reviews* 92, no. 1: 101–130. https://doi.org/10.1152/physrev.00021.2011.

Kahn, S., Y. Liao, X. Du, W. Xu, J. Li, and B. Lönnerdal. 2018. "Exosomal MicroRNAs in Milk From Mothers Delivering Preterm Infants Survive In Vitro Digestion and Are Taken up by Human Intestinal Cells." *Molecular Nutrition & Food Research* 62, no. 11: 1701050. https://doi.org/10.1002/mnfr.201701050.

Kunz, C., and B. Lönnerdal. 1989. "Human Milk Proteins: Separation of Whey Proteins and Their Analysis by Polyacrylamide Gel Electrophoresis, Fast Protein Liquid Chromatography (FPLC) Gel Filtration, and Anion-Exchange Chromatography." *American Journal of Clinical Nutrition* 49, no. 3: 464–470. https://doi.org/10.1093/ajcn/49.3.464.

Li, C. M.-C., H. Shapiro, C. Tsiobikas, et al. 2020. "Aging-Associated Alterations in Mammary Epithelia and Stroma Revealed by Single-Cell RNA Sequencing." *Cell Reports* 33, no. 13: 108566. https://doi.org/10.1016/j.celrep.2020.108566.

Li, W.-J., H. Chen, M.-L. Tong, J.-J. Niu, X.-Z. Zhu, and L.-R. Lin. 2022. "Comparison of the Yield and Purity of Plasma Exosomes Extracted by Ultracentrifugation, Precipitation, and Membrane-Based Approaches." *Open Chemistry* 20, no. 1: 182–191. https://doi.org/10.1515/chem-2022-0139.

Liangsupree, T., E. Multia, and M.-L. Riekkola. 2021. "Modern Isolation and Separation Techniques for Extracellular Vesicles." *Journal of Chromatography A* 1636: 461773. https://doi.org/10.1016/j.chroma.2020.461773.

Liao, Y., X. Du, J. Li, and B. Lönnerdal. 2017. "Human Milk Exosomes and Their microRNAs Survive Digestion In Vitro and Are Taken up by Human Intestinal Cells." *Molecular Nutrition & Food Research* 61, no. 11: 1700082. https://doi.org/10.1002/mnfr.201700082.

Lönnerdal, B. 2003. "Nutritional and Physiologic Significance of Human Milk Proteins." *American Journal of Clinical Nutrition* 77, no. 6: 1537S–1543S. https://doi.org/10.1093/ajcn/77.6.1537S.

Lynes, M. D., L. O. Leiria, M. Lundh, et al. 2017. "The Cold-Induced Lipokine 12,13-diHOME Promotes Fatty Acid Transport Into Brown Adipose Tissue." *Nature Medicine* 23, no. 5: 631–637. https://doi.org/10.1038/nm.4297.

Macêdo, A. P. A., V. R. Muñoz, D. E. Cintra, and J. R. Pauli. 2022. "12,13-diHOME as a New Therapeutic Target for Metabolic Diseases." *Life Sciences* 290: 120229. https://doi.org/10.1016/j.lfs.2021.120229.

Melero-Fernandez de Mera, R., A. Villaseñor, D. Rojo, et al. 2022. "Ceramide Composition in Exosomes for Characterization of Glioblastoma Stem-Like Cell Phenotypes." *Frontiers in Oncology* 11: 788100. https://doi.org/10.3389/fonc.2021.788100.

Morisseau, C., and B. D. Hammock. 2013. "Impact of Soluble Epoxide Hydrolase and Epoxyeicosanoids on Human Health." *Annual Review of Pharmacology and Toxicology* 53, no. 1: 37–58. https://doi.org/10.1146/annurev-pharmtox-011112-140244.

Neville, M. C., J. Morton, and S. Umemura. 2001. "Lactogenesis: The Transition From Pregnancy to Lactation." *Pediatric Clinics of North America* 48, no. 1: 35–52. https://doi.org/10.1016/S0031-3955(05)70284-4.

Niño, D. F., C. P. Sodhi, and D. J. Hackam. 2016. "Necrotizing Enterocolitis: New Insights Into Pathogenesis and Mechanisms." *Nature Reviews Gastroenterology & Hepatology* 13, no. 10: 590–600. https://doi.org/10.1038/nrgastro.2016.119.

Nordin, J. Z., Y. Lee, P. Vader, et al. 2015. "Ultrafiltration With Size-Exclusion Liquid Chromatography for High Yield Isolation of Extracellular Vesicles Preserving Intact Biophysical and Functional Properties." *Nanomedicine: Nanotechnology, Biology and Medicine* 11, no. 4: 879–883. https://doi.org/10.1016/j.nano.2015.01.003.

Oeyen, E., K. Van Mol, G. Baggerman, et al. 2018. "Ultrafiltration and Size Exclusion Chromatography Combined With Asymmetrical-Flow Field-Flow Fractionation for the Isolation and Characterisation of Extracellular Vesicles From Urine." *Journal of Extracellular Vesicles* 7, no. 1: 1490143. https://doi.org/10.1080/20013078.2018.1490143.

Panigrahy, D., B. T. Kalish, S. Huang, et al. 2013. "Epoxyeicosanoids Promote Organ and Tissue Regeneration." *Proceedings of the National Academy of Sciences of the United States of America* 110, no. 33: 13528–13533. https://doi.org/10.1073/pnas.1311565110.

Pisano, C., J. Galley, M. Elbahrawy, et al. 2020. "Human Breast Milk-Derived Extracellular Vesicles in the Protection against Experimental Necrotizing Enterocolitis." *Journal of Pediatric Surgery* 55, no. 1: 54–58. https://doi.org/10.1016/j.jpedsurg.2019.09.052.

Rahman, M. M., K. Shimizu, M. Yamauchi, et al. 2019. "Acidification Effects on Isolation of Extracellular Vesicles From Bovine Milk." *PLoS ONE* 14, no. 9: e0222613.

Ramos-Garcia, V., I. Ten-Doménech, A. Moreno-Giménez, et al. 2021. "ATR-FTIR Spectroscopy for the Routine Quality Control of Exosome Isolations." *Chemometrics and Intelligent Laboratory Systems* 217: 104401.

Robinson, S. D., M. Samuels, W. Jones, D. Gilbert, G. Critchley, and G. Giamas. 2023. "Shooting the Messenger: A Systematic Review Investigating Extracellular Vesicle Isolation and Characterisation Methods and Their Influence on Understanding Extracellular Vesicles-Radiotherapy Interactions in Glioblastoma." *BMC Cancer* 23, no. 1: 939. https://doi.org/10.1186/s12885-023-11437-6.

Schedin, P., and P. J. Keely. 2011. "Mammary Gland ECM Remodeling, Stiffness, and Mechanosignaling in Normal Development and Tumor

27682811, 2026, 1, Downloaded from https://iseojournals.onlinelibrary.wiley.com/doi/10.1002/jex2.70110 by Spanish Cochrane National Provision (Ministerio de Sanidad), Wiley Online Library on [11/03/2026]. See the Terms and Conditions (https://onlinelibrary.wiley.com/terms-and-conditions) on Wiley Online Library for rules of use; OA articles are governed by the applicable Creative Commons License

Progression." *Cold Spring Harbor Perspectives in Biology* 3, no. 1: a003228–a003228. https://doi.org/10.1101/cshperspect.a003228.

Serhan, C. N., and B. D. Levy. 2018. "Resolvins in Inflammation: Emergence of the Pro-Resolving Superfamily of Mediators." *Journal of Clinical Investigation* 128, no. 7: 2657–2669. https://doi.org/10.1172/JCI97943.

Sidhom, K., P. O. Obi, and A. Saleem. 2020. "A Review of Exosomal Isolation Methods: Is Size Exclusion Chromatography the Best Option?" *International Journal of Molecular Sciences* 21, no. 18: 6466. https://doi.org/10.3390/ijms21186466.

Simon, T., A. Kumaran, D.-F. Veselu, and G. Giamas. 2020. "Three Method-Combination Protocol for Improving Purity of Extracellular Vesicles." *International Journal of Molecular Sciences* 21, no. 9: 3071. https://doi.org/10.3390/ijms21093071.

Sokolova, V., A.-K. Ludwig, S. Hornung, et al. 2011. "Characterisation of Exosomes Derived From Human Cells by Nanoparticle Tracking Analysis and Scanning Electron Microscopy." *Colloids and Surfaces B, Biointerfaces* 87, no. 1: 146–150. https://doi.org/10.1016/j.colsurfb.2011.05.013.

Spector, A. A., and A. W. Norris. 2007. "Action of Epoxyeicosatrienoic Acids on Cellular Function." *American Journal of Physiology-Cell Physiology* 292, no. 3: C996–C1012. https://doi.org/10.1152/ajpcell.00402.2006.

Takov, K., D. M. Yellon, and S. M. Davidson. 2019. "Comparison of Small Extracellular Vesicles Isolated From Plasma by Ultracentrifugation or Size-Exclusion Chromatography: Yield, Purity and Functional Potential." *Journal of Extracellular Vesicles* 8, no. 1: 1560809. https://doi.org/10.1080/20013078.2018.1560809.

Ten-Doménech, I., E. F. Simó-Alfonso, and J. M. Herrero-Martínez. 2018. "Improving Fractionation of Human Milk Proteins Through Calcium Phosphate Coprecipitation and Their Rapid Characterization by Capillary Electrophoresis." *Journal of Proteome Research* 17, no. 10: 3557–3564.

Ter-Ovanesyan, D., M. Norman, R. Lazarovits, et al. 2021. "Framework for Rapid Comparison of Extracellular Vesicle Isolation Methods." *eLife* 10: e70725. https://doi.org/10.7554/eLife.70725.

Tong, L., S. Zhang, Q. Liu, et al. 2023. "Milk-Derived Extracellular Vesicles Protect Intestinal Barrier Integrity in the Gut-Liver Axis." *Science Advances* 9, no. 15: eade5041. https://doi.org/10.1126/sciadv.ade5041.

Vahkal, B., I. Altosaar, A. Ariana, et al. 2024. "Human Milk Extracellular Vesicles Modulate Inflammation and Cell Survival in Intestinal and Immune Cells." *Pediatric Research* 98: 314–326. https://doi.org/10.1038/s41390-024-03757-5.

EV-TRACK Consortium. Van Deun, J., P. Mestdagh, et al. 2017. "EV-TRACK: Transparent Reporting and Centralizing Knowledge in Extracellular Vesicle Research." *Nature Methods* 14, no. 3: 228–232. https://doi.org/10.1038/nmeth.4185.

Van Herwijnen, M. J. C., M. I. Zonneveld, S. Goerdayal, et al. 2016. "Comprehensive Proteomic Analysis of Human Milk-Derived Extracellular Vesicles Unveils a Novel Functional Proteome Distinct From Other Milk Components." *Molecular & Cellular Proteomics* 15, no. 11: 3412–3423. https://doi.org/10.1074/mcp.M116.060426.

Wang, L., G. Luo, L.-F. Zhang, and H.-X. Geng. 2018. "Neuroprotective Effects of Epoxyeicosatrienoic Acids." *Prostaglandins & Other Lipid Mediators* 138: 9–14. https://doi.org/10.1016/j.prostaglandins.2018.07.002.

Wang, X., X. Yan, L. Zhang, et al. 2019. "Identification and Peptidomic Profiling of Exosomes in Preterm Human Milk: Insights into Necrotizing Enterocolitis Prevention." *Molecular Nutrition & Food Research* 63, no. 13: 1801247. https://doi.org/10.1002/mnfr.201801247.

Webber, J., and A. Clayton. 2013. "How Pure Are Your Vesicles?" *Journal of Extracellular Vesicles* 2, no. 1: 19861. https://doi.org/10.3402/jev.v2i0.19861.

Welsh, J. A., D. C. I. Goberdhan, L. O'Driscoll, et al. 2024. "Minimal Information for Studies of Extracellular Vesicles (MISEV2023): From Basic to Advanced Approaches." *Journal of Extracellular Vesicles* 13, no. 2: e12404. https://doi.org/10.1002/jev2.12404.

Yamauchi, M., K. Shimizu, M. Rahman, et al. 2019. "Efficient Method for Isolation of Exosomes From Raw Bovine Milk." *Drug Development and Industrial Pharmacy* 45, no. 3: 359–364. https://doi.org/10.1080/03639045.2018.1539743.

Yan, X., L. Liu, S. Yao, et al. 2022. "LncRNA and mRNA Profiles of Human Milk-Derived Exosomes and Their Possible Roles in Protecting Against Necrotizing Enterocolitis." *Food & Function* 13, no. 24: 12953–12965. https://doi.org/10.1039/D2FO01866G.

Yuana, Y., J. Levels, A. Grootemaat, A. Sturk, and R. Nieuwland. 2014. "Co-isolation of Extracellular Vesicles and High-density Lipoproteins Using Density Gradient Ultracentrifugation." *Journal of Extracellular Vesicles* 3, no. 1: 23262. https://doi.org/10.3402/jev.v3.23262.

Yung, C., Y. Zhang, M. Kuhn, et al. 2024. "Neonatal Enteroids Absorb Extracellular Vesicles From Human Milk-Fed Infant Digestive Fluid." *Journal of Extracellular Vesicles* 13, no. 4: e12422. https://doi.org/10.1002/jev2.12422.

Zhou, Q., M. Li, X. Wang, et al. 2012. "Immune-Related MicroRNAs Are Abundant in Breast Milk Exosomes." *International Journal of Biological Sciences* 8, no. 1: 118–123. https://doi.org/10.7150/ijbs.8.118.

Supporting Information

Additional supporting information can be found online in the Supporting Information section.

Supporting Information: jex270110-sup-0001-SuppMat.docx

27682811, 2026, 1, Downloaded from https://isevjournals.onlinelibrary.wiley.com/doi/10.1002/jex2.70110 by Spanish Cochrane National Provision (Ministerio de Sanidad), Wiley Online Library on [11/03/2026]. See the Terms and Conditions (https://onlinelibrary.wiley.com/terms-and-conditions) on Wiley Online Library for rules of use; OA articles are governed by the applicable Creative Commons License